RAPID COMMUNICATIONS

PHYSICAL REVIEW B VOLUME 50, NUMBER 9 1 SEPTEMBER 1994-I

Spectroscopic manifestation of a confinement-type lattice anharmonicity

M. Grinberg, W. Jaskólski, Cz. Koepke, J. Planelles,* and M. Janowicz
Instytut Fizyki, Uniwersytet Mikołaja Kopernika, Grudziądzka 5, 87-100 Toruń, Poland
(Received 4 April 1994)

The observed broadening of the line shape of the emission spectra of the luminescence centers in crystals with high electron-lattice coupling has been explained in terms of the ion-motion spatial confinement in the lattice. For this, a simple and analytically solvable model for the potential of the electronic energy sheets has been proposed. As an example of application the emission spectrum of BiO_6^{9-} complex has been analyzed.

In the theoretical description of the emission and absorption spectra of the luminescence centers in crystals, the standard and most widely used approach[1] assumes that both the excited and the ground electronic manifolds are represented by the energy sheets generated by the elastic forces. In the totally symmetrical vibronic mode, this corresponds to one-dimensional shifted parabolas. The whole spectral line shape of the transitions between various phonon states is reproduced by the sequence of squares of overlap integrals between the vibronic wave functions of the initial and final electronic states. The emission and absorption spectra are given by the Pekarian curve:[2,3]

$$I(E)=\exp(-S)\frac{S^n}{n!}\,\delta(E-(\epsilon_0-n\hbar\omega)). \tag{1}$$

Here S is the Hung and Rhys factor, ϵ_0 is the energy of the zero-phonon line, and $\hbar\omega$ is the energy of phonon. This model works well for small and medium electron-lattice couplings (S is of the order of unity, in general smaller than ten).[5] For large couplings, however, when the Hung and Rhys factor is greater than ten, like in color centers[6] or in metal complexes,[7] the individual lines corresponding to transitions to various excited phonon states are broadened and cannot be detected. In such a case, formula (1) cannot be verified directly and all the parameters of the system should be detected from the whole spectrum line shape. Since in that case the offset between the ground and excited electronic manifolds is very large, one should verify assumptions concerning the lattice potential for large displacements of the ions. We are concerned in particular about the assumption of the lattice elasticity, which yields the vibronic Hamiltonian proportional to the square of the ionic displacement in the whole range of displacements considered here. The knowledge about the shape of the energy sheets is very important, since in many cases the interpretation of the spectra by the standard harmonic oscillator approach is ambiguous and results in unexpected energy of the zero-phonon line, and in very large energy of phonons (this problem will be discussed further in more detail). Similar problems may occur in the interconfigurational nonradiative internal conversion processes. In such a case, the calculated probability of the nonradiative transitions induced by the crossing of the displaced ground and excited energy sheets requires also a very large phonon energy to fit the theoretical predictions to the experimental data.[2] One can extend the model to consider interactions with more than one vibronic mode, as well as "square" contributions to the electron-lattice coupling. For example, in the case of the Al_2O_3:Ti^3 system this procedure was successful.[4] Nevertheless, when we do not have the specific structure of the spectrum suggesting a large static Jahn-Teller distortion, such a procedure may not be essential.

It has been shown recently[8] that the characteristic features (like, e.g., spectra) of many physical systems may change considerably when the system becomes spatially confined. In many cases (impurity states in low-dimensional semiconductor structures or atoms and molecules in molecular zeolite sieves) the spatial confinement is frequently described by the model of a potential well with infinite barriers.[8–10] It is rather obvious that for ionic vibrations in lattice, a deviation from the free parabolic potential may be modeled by putting high potential barriers related to the rigid host lattice, which confines the motion of ions.

In this paper we present a model potential, which takes into account spatial confinement of the ionic motion. We then use it in order to reproduce the experimental broad band emission luminescence spectrum of BiO_6^{9-} complex in $Bi_4Ge_3O_{12}$ (BGO) crystal. The results are compared with the ones obtained by using the harmonic lattice potential model, and we find our approach much more reasonable. The confined potential, which we use, enables us to explain in a simple way the experimentally observed broadening of the spectrum line shape.

The material we have used to observe the emission spectra was chosen from crystals and glasses with molecular complexes as the emitting centers.[11–13,18] The complexes consist of a central metal ion and oxygen ligands in the four- or the six-fold coordination in O_h or T_d symmetry, respectively, in the ideal case. All such systems are characterized by broad absorption and emission bands resulting from the strong electron-lattice coupling. In the materials considered, the emission is spin forbidden and occurs from the lowest triplet term of the excited configuration.[14,15] We deal thus with two different zero-phonon lines, one for emission and the other for absorption (occurring to one of the singlets of the excited configuration). The zero-phonon line for the emission is, therefore, expected to lie in the high-energy tail of the emission spectrum (instead of lying between the emission and the absorption maxima) and falls within 26 000–28 000 cm^{-1} interval for the material used here. However, the strong electron-phonon coupling makes this line very hard to detect, and in consequence, it is invisible even at low

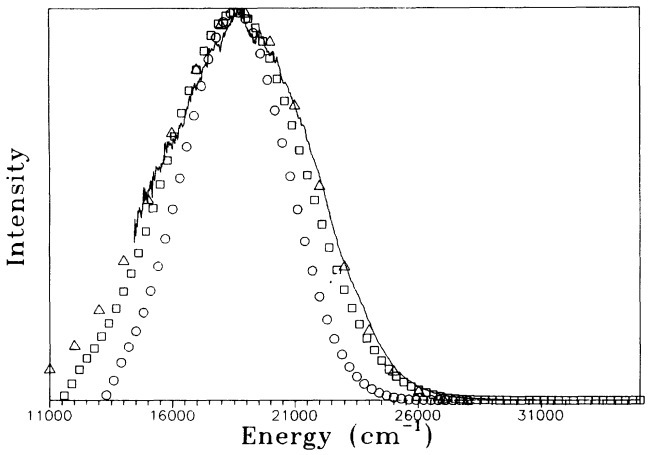

FIG. 1. Three attempts of fitting to the emission spectrum of BiO_6^{9-} complex, obtained using the standard approach. Solid curve: experimental spectral line shape; triangles (a): $\epsilon_0=28\ 000\ cm^{-1}$, $\hbar\omega=1000\ cm^{-1}$; rectangles (b): $\epsilon_0=35\ 000\ cm^{-1}$, $\hbar\omega=300\ cm^{-1}$; circles (c): $\epsilon_0=28\ 000\ cm^{-1}$, $\hbar\omega=300\ cm^{-1}$.

temperatures.[16] The spectra of these materials exhibit some common features. They are broad, structureless, and often have very similar shapes. We expect that the effect of anharmonicity on the potential energy curves, which we explain in one example, manifests itself in all of the emission spectra reported.[12,13,18]

The experimental setup, involving the optical multichannel analyzer as a detector and the excimer laser (XeCl) working at 308 nm as a source of excitation, was described in Ref. 13. The experimental line shapes are to be compared with theoretical predictions for the shapes of the emission rate distributions. To do this, all the measured spectra were transformed to the line shape form according to procedure described in details in Ref. 17.

As an example we have considered the emission spectrum of BiO_6^{9-} complex in BGO crystal. (It is important to note, that the optical properties of this stoichiometric material are solely determined by the considered complex. In contrast to glasses with molecular complexes, where the crystal field distribution can alter the emission spectrum, the BGO crystal exhibits one-site emission and is a proper candidate for our considerations. This one-site character of the emission has been confirmed by a single-exponential decay of the luminescence.[12]) The experimental spectrum is shown in Fig. 1. Three different attempts to fit the theoretical curve, obtained in standard harmonic oscillator approach, to the experimental emission line shape are also presented. Since the experimental spectrum have been observed in the room temperature, the emission from higher vibronic states of the excited electronic manifold is also considered, and instead of using formula (1) we have

$$I(E)=\sum_{n,m}|\langle e,m|g,n\rangle|^2 f(E_m)\,\delta\{E-[\epsilon_0-(n-m)\hbar\omega]\}, \tag{2}$$

where $|g,n\rangle$ and $|e,m\rangle$ are harmonic oscillator wave functions representing vibronic states of the ground and excited electronic manifolds, and $f(E_n)$ is the Boltzmann occupation

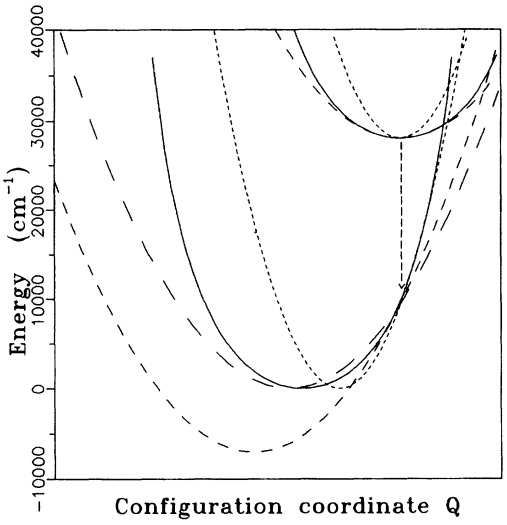

FIG. 2. Configuration coordinate diagrams for BiO_6^{9-} complex resulting from the fitting procedures. Solid line: present model potential. Other lines correspond to cases (a), (b), and (c) as in Fig. 1: dotted line (a), dashed (short) (b), dashed (long) (c)—coincides with (b) for the upper curve (the same $\hbar\omega$). Vertical arrow corresponds to the transitions in the maximum of the emission line shape.

number. The overlap integrals were calculated according to the recurrence formula described in Ref. 3. The zero-phonon line energy ϵ_0 and the phonon energy $\hbar\omega$ are the only free parameters in the fitting procedure. For a reasonable phonon energy ($300\ cm^{-1}$), the value for the zero-phonon line required to make the best fit is rather unphysical ($35\ 000\ cm^{-1}$) Ref. 19, and falls near the first maximum of the absorption spectrum (the curve represented by rectangles). On the other hand, when we chose a realistic $\epsilon_0=28\ 000\ cm^{-1}$, an unacceptable value of $\hbar\omega=1000\ cm^{-1}$ has to be taken (triangles) to obtain a reasonable fit. Choosing realistic values for both ϵ_0 and $\hbar\omega$ ($28\ 000\ cm^{-1}$ and $300\ cm^{-1}$, respectively), results in a bad fit, represented in Fig. 1 by circles. The electron energy sheet diagrams are presented, for illustration, in Fig. 2 (dashed and dotted curves). Similar results have been obtained when we analyzed the emission spectra of other crystals and glasses.[13,18] The presented results show that the usual procedure of fitting the emission line shape fails in the presence of strong electron-phonon coupling. It means that the assumption about harmonic oscillations for high vibronic states and in the whole range of displacements is too simplistic in the case of optically active ions in such materials. We thus propose here another model, which in the frame of a single fully symmetrical "breathing" mode goes beyond the simple harmonic oscillator picture by taking into account the confinement of the ionic motion in lattice, but retains simultaneously its analytical simplicity.

Before we discuss our model potential let us have a look at another system, which shows the broad vibronic absorption and emission bands. In a diatomic molecule the energy sheets are usually approximated by the Morse potential (see Fig. 3, asterisks), which increase to infinity when the atoms are close to each other, and falls to zero when they are far apart. Although in the vicinity of the minimum the potential

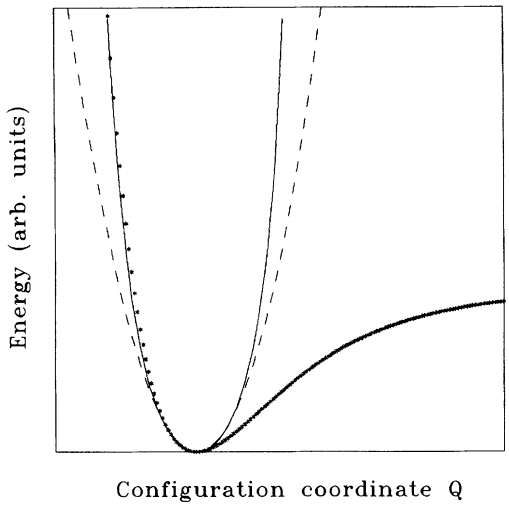

FIG. 3. Various types of vibronic potentials; dashed curve: harmonic lattice; asterisks: Morse potential; solid curve: our model potential.

can be described by a parabola, for higher energies it is strongly anharmonic. In the case of a solid state we consider the system of complex ion which consists of the central metal ion and four or six oxygen ligands surrounded by the other host ions. Thus, when the local vibrations are considered, large displacements of an arbitrary ion are limited by the presence of its neighbors. Not taking into account the special case when the ion migration is allowed, an arbitrary deflection of the individual ion leading to dissociation is rather unexpected. For this reason we assume that for large ionic displacements in any direction, the potential increases more rapidly than the harmonic one. One can study different types of anharmonicity yielding contraction of the potential energy curve. One possibility is, for example, the harmonic oscillator potential embedded in the infinite rectangular well; another one is an anharmonicity proportional to the fourth power of the displacement variable.

We propose here a model, which gives analytical solutions having simple physical interpretation. The solutions of our model potential fulfill simple recurrence relation, and can be easily generated to any required order. The potential has special importance in the calculation of the spectral line shape, where vibronic wave functions for highly excited phonons are currently required. One has to stress that such a calculation and theoretical prediction of the spectrum could not be done if one were condemned to perform exact integration of the Schrödinger equation in order to obtain the high-lying states. In our model the Schrödinger equation for the totally symmetrical mode of vibration reads

$$\left(-\frac{1}{2}\frac{d^2}{dQ^2}+V_\alpha(Q)+E_n\right)\Psi^n(Q)=0, \tag{3}$$

where Q is the configurational generalized coordinate, and

$$V_\alpha(Q)=\frac{\alpha(\alpha-1)}{2\sin^2 Q} \tag{4}$$

is a model potential (Figs. 2 and 3, solid line), which extends [the confining region can be declared as $(0-a)$, for arbitrary a, by a simple substitution $\tilde{Q}=Q\pi/a$] from 0 to π, and $V(Q)\to\infty$ for $Q\to 0$ and $Q\to\pi$. The energy E_n, with respect to the bottom of the potential is

$$E_n=\frac{n^2}{2}+\alpha(n+\tfrac{1}{2}), \quad n=0,1,2\ldots \tag{5}$$

and the solutions of Eq. (3), corresponding to $|g,n\rangle$ vibronic states, have the form:

$$\Psi_{n,\alpha}(Q)=\sin^\alpha(Q)C_n^{(\alpha)}[\cos(Q)], \tag{6}$$

where $C_n^{(\alpha)}[\cos(Q)]$ are Gegenbauer polynomials.[20] The wave functions $\Psi_{n,\alpha}(Q)$ vanish at the border of the confining region, i.e., where the potential $V_\alpha(Q)\to\infty$. For further comparison with the harmonic oscillator solutions, let us denote as $\frac{1}{2}\hbar\omega$ the energy of the ground state $E_0=\frac{1}{2}\alpha$. For small ionic displacements around the equilibrium position $Q=\pi/2$, the potential becomes $V_\alpha\approx[\alpha(\alpha-1)/2](Q-\pi/2)^2$, and is a good approximation to the harmonic oscillator potential. As the effect of the spatial confinement, the energies E_n are not equally spaced, and $E_{n+1}-E_n=[1+(n+\frac{1}{2})/\alpha]\hbar\omega$. For $\alpha\gg 1$ and n not too large, i.e., near the bottom of the potential, $E_{n+1}-E_n\approx\hbar\omega$.

The excited state potential curve has to be shifted in the energy scale by the amount ϵ_0 corresponding to the zero-phonon line, and by δ in Q variable in order to represent the different equilibrium position due to the electron-lattice coupling. Various shapes of the potential curve may be chosen by different parametrization α, and finally the potential for the excited states is

$$V_{\alpha'}(Q-\delta)+\epsilon_0. \tag{7}$$

Let us denote the vibronic wave functions corresponding to the $|e,m\rangle$ state of the excited electronic manifold as $\Psi_{m,\alpha'}(Q)$. The transition probabilities $P_{n\alpha,m\alpha'}$ between different phonon states (n,m) belonging to the ground (α) and excited (α') electron states are in this model proportional to the squares of the corresponding functions. The emission spectral line shape for transitions from m to various (n) phonon states of the final (ground) electron state reads

$$I_{m,n}(E)=\left|\int_\delta^\pi \Psi^*_{n,\alpha}(Q)\Psi_{m,\alpha'}(Q)dQ\right|^2\delta[E-(E_m-E_n)]. \tag{8}$$

For the temperature 0 K, the transitions are assumed to occur from the $m=0$ vibronic state of the excited electron state. For higher temperatures $\Gamma>0$ K, one has to perform summation over all $I_{m,n}$ [see Eq. (2)], and the final spectrum line shape is given by

$$I(E)=\sum_{m,n} I_{m,n}(E)f(E_m). \tag{9}$$

We have performed calculations considering α as a free adjustable parameter of the system. Very good fits to the experimental spectrum have been obtained for $\alpha=\alpha'=127.1$ and $\delta=0.62$. This corresponds to realistic $\epsilon_0=28\,000$ cm^{-1} and $\hbar\omega=300$ cm^{-1}. The results are pre-

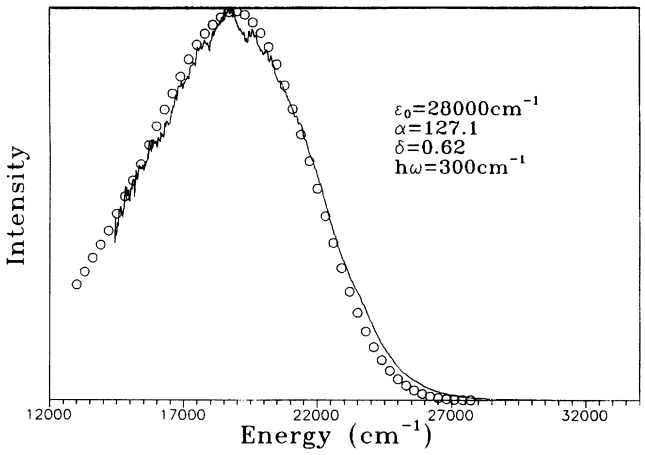

FIG. 4. Theoretical fit (circles) to the emission spectrum of BiO_6^{9-} complex obtained using the model potential defined by Eqs. (4) and (7) $\epsilon_0=28\,000$ cm^{-1}, $\hbar\omega=300$ cm^{-1}, $\alpha=127.1$, and $\delta=0.62$.

sented in Fig. 4. Comparing the results presented in Figs. 1 and 4 one can see that the assumption of the ionic motion confinement yields much better fit to the experimental emission line shape than the standard approach.

The intensity of the emission from the mth $|e,m\rangle$ vibronic state of the excited electronic manifold can be rewritten in the form: $I_m(E)=\Sigma_n\langle e,m|W_n|e,m\rangle$. The operator W_n is given by $W_n=|g,n\rangle\langle g,n|\delta[E-(E_m-E_n)]f(E_m)$ and determines the line shape in two ways: by the dependence on the energetic structure, and by the dependence on the vibronic wave functions related to the ground electronic manifold. The former dependence has "nonlocal" character, since it is the consequence of the potential shape in the whole range of the displacement variable Q, whereas the latter one is "local," because it concerns only the range of Q near the bottom of the excited state energy sheet. Comparing the results of our model potential calculations with the ones obtained using the harmonic oscillator approach, one can see that in the confined case the line shape is much broader, and exhibits slight asymmetric broadening in the range corresponding to transitions to higher vibronic states. The broadening is due to the energetic distance between the neighboring vibronic states, which increases slowly in the confined case, while it is constant in the harmonic oscillator case. This effect is additionally enhanced by moderate changes resulting from the potential curvature (accumulation of the main maxima of the wave functions near the border of the confining region).

The luminescence spectra were taken during the program aimed at evaluation of potential laser characteristics of molecular ions in solids, conducted by Professor A. Lempicki, at Boston University.

*Departament de Ciències Experimentals, Universitat Jaume I, Apartat 224, 12080 Castelló, Spain.

[1] K. Hung and A. Rhys, Proc. R. Soc. London **A204**, 406 (1950).
[2] C W. Struck and W. H. Fonger, J. Lumin. **10**, 1 (1975).
[3] C. Manneback, Physica **17**, 1001 (1951).
[4] M. Grinberg, A. Mandelis, and K. Fjeldsted, Phys. Rev. B **48**, 5935 (1993).
[5] P.T. Kenyon, L. Andrews, M. Mc Collum, and A. Lempicki, IEEE J. Quantum Electron. **18**, 1189 (1982).
[6] W.B. Fowler, in *Physics of Color Centers*, edited by W.B. Fowler (Academic, New York, 1968), p. 54.
[7] G. Blasse, Struct. Bonding (Berlin) **42**, 1 (1980).
[8] C. Zicovich-Wilson, J. Planelles, and W. Jaskólski, Int. J. Quantum Chem. **50**, 429 (1994).
[9] A.F. Kovalenko, E.N. Sovyak, and M.F. Holovko, Int. J. Quantum Chem. **42**, 321 (1992).
[10] J.L. Zhu, J.J. Xiong, and B.L. Gu, Phys. Rev. B **41**, 6001 (1990).
[11] Cz. Koepke and A. Lempicki, Chem. Phys. Lett. **172**, 224 (1990).
[12] Cz. Koepke and A. Lempicki, Chem. Phys. Lett. **172**, 227 (1990).
[13] Cz. Koepke, A.J. Wojtowicz, and A. Lempicki, J. Lumin. **54**, 345 (1993).
[14] W. Barendswaard, R.T. Weber, and J.H. van der Waals, J. Chem. Phys. **87**, 3731 (1987).
[15] R. Moncorgé, B. Jacquier, G. Boulon, F. Gaume-Mahn, and J. Janin, J. Lumin. **12/13**, 467 (1976).
[16] C.C. Klick, J. Opt. Soc. Am. **41**, 816 (1951).
[17] A. Wojtowicz, M. Kaźmierczak, A. Lempicki, and R. H. Bartram, J. Opt. Soc. Am. **6**, 1106 (1989).
[18] Cz. Koepke, A. Lempicki, and G. H. Beall, J. Lumin. **54**, 145 (1992); **54**, 151 (1992).
[19] R. Moncorgé, B. Jacquier, and G. Boulon, J. Lumin. **14**, 337 (1976).
[20] *Handbook of Mathematical Functions*, edited by M. Abramowitz and I.A. Stegun (Dover, New York, 1965).